Virus Research 261 (2019) 37–49

Contents lists available at ScienceDirect

Virus Research

journal homepage: www.elsevier.com/locate/virusres

The bovine herpesvirus-1 major tegument protein, VP8, interacts with host HSP60 concomitant with deregulation of mitochondrial function

Sharmin Afroz[a,b], Robert Brownlie[a], Michel Fodje[c], Sylvia van Drunen Littel-van den Hurk[a,b,d,*]

[a] VIDO-InterVac, University of Saskatchewan, Saskatoon, SK, S7N 5E3, Canada
[b] Vaccinology & Immunotherapeutics, University of Saskatchewan, Saskatoon, SK, S7N 2Z4, Canada
[c] Canadian Light Source, University of Saskatchewan, Saskatoon, SK, S7N 2V3, Canada
[d] Microbiology & Immunology, University of Saskatchewan, Saskatoon, SK, S7N 5E5, Canada

ARTICLE INFO

Keywords:
BoHV-1
VP8
HSP60
Mitochondria

ABSTRACT

The U_L47 gene product, VP8, is a major tegument protein of BoHV-1. While VP8 is not essential for virus replication in cell culture, a U_L47-deleted virus exhibits a smaller tegument structure and is avirulent in cattle. To obtain pure VP8 protein for structural analysis, we expressed a N-terminally truncated version of VP8 in *Eschericia coli.* However, the recombinant VP8 was consistently co-purified with a tightly associated bacterial protein; this protein was identified by mass spectrometry as GroEL, which has considerable homology with mammalian heat shock protein-60 (HSP60), thus suggesting a new role for VP8 in virus-host interaction. A physical interaction of HSP60 and VP8 in both VP8-transfected and BoHV-1-infected cells was demonstrated by immunoprecipitation. Analysis of different truncated VP8 constructs revealed that amino acids 259–482 and 632–741 are involved in binding to HSP60. Full-length VP8 and VP8 219–741 (containing both interacting domains, 259–482 and 632–741) co-localized with HSP60 and mitochondria. VP8 was localized in the mitochondria from 2 to 14 h post infection in BoHV-1-infected cells. The mitochondrial membrane potential was reduced in both VP8-transfected and BoHV-1-infected cells and was further diminished by overexpression of HSP60 in the presence of VP8. In addition, VP8 expression decreased the ATP concentration during transfection, as well as BoHV-1 infection. Thus, VP8 may play a role in the deregulation of mitochondrial function through interaction with HSP60. This is consistent with the fact that BoHV-1 infection is known to promote mitochondrial dysfunction.

1. Introduction

Bovine herpesvirus-1 (BoHV-1) is an alpha herpesvirus and a major pathogen in cattle (Jones and Chowdhury, 2007; Roizman et al., 1981), causing several diseases, including conjunctivitis, infectious bovine rhinotracheitis, balanoposthitis and abortions. Thus, BoHV-1 contributes to significant economic losses to the North American cattle industry (Jones and Chowdhury, 2007). BoHV-1 is a double-stranded DNA virus with a ~140 kb genome. It contains four different compartments; a DNA core enclosed within a capsid, a thick tegument layer and an outer envelope with glycoproteins (Mettenleiter et al., 2009). The tegument of the BoHV-1 virion is the most complex structure containing ~ 20 virus-encoded proteins. The functions of the proteins in the tegument are not well understood. In addition to their structural role, tegument proteins contribute to multiple regulatory functions including DNA replication, transcriptional regulation, capsid transport, and kinase activity (Kelly et al., 2009). Hence, the tegument proteins play a significant role during the establishment of virus infection.

The U_L47 gene product, VP8, is the most abundant tegument protein of BoHV-1 (Carpenter and Misra, 1991). VP8 is not essential for viral replication *in vitro*. However, a U_L47-deleted BoHV-1 mutant has a smaller tegument structure and does not replicate in cattle (Lobanov et al., 2010). VP8 contains a nuclear localization signal (NLS) and at least two nuclear export signals (NESs), which are responsible for shuttling of VP8 between the cytoplasm and nucleus (Verhagen et al., 2006; Zheng et al., 2004). Early during infection the virion VP8 and the *de novo* synthesized VP8 can be detected in the cytoplasm. With the progression of infection VP8 localizes to the nucleus and later during infection VP8 is again observed in the cytoplasm (van Drunen Littel-van den Hurk et al., 1995; Vasilenko et al., 2012). VP8 has also been detected in the cisternae of the Golgi and found to interact with gB, gC, and gD mRNAs (Islam et al., 2015; van Drunen Littel-van den Hurk

* Corresponding author at: VIDO-InterVac, University of Saskatchewan, 120 Veterinary Road, Saskatoon, SK, S7N 5E3, Canada.
E-mail address: sylvia.vandenhurk@usask.ca (S. van Drunen Littel-van den Hurk).

https://doi.org/10.1016/j.virusres.2018.12.006
Received 2 August 2018; Received in revised form 10 December 2018; Accepted 11 December 2018
Available online 11 December 2018
0168-1702/ © 2018 Elsevier B.V. All rights reserved.

et al., 1995).

VP8 is a multifunctional protein and is extensively involved in host-pathogen interactions. BoHV-1 VP8 interacts with cellular CK2 and viral US3 kinase (Labiuk et al., 2009). Recently, it has been demonstrated that phosphorylated VP8 redistributes promyelocytic leukemia (PML) (Zhang et al., 2015). Furthermore, VP8 interacts with DNA damage-binding protein-1 (DDB1) (Vasilenko et al., 2012) and with the cellular signal transducer and activator of transcription (STAT1) to down-regulate interferon-β (IFN-β) signaling (Afroz et al., 2016). Recently, we demonstrated that VP8 induces apoptosis and increases DNA damage-induced apoptosis (Afroz et al., 2018). Homologues of VP8 are present in different herpesviruses, such as VP13/14 herpes simplex virus-1^{-1} (HSV-1). The C-terminal domain of VP8 is enriched with alpha-helical structures and is conserved among some herpesviruses (Afroz et al., 2016).

Heat shock protein-60 (HSP60), a molecular chaperone, is involved in correct folding of a protein or degradation of a misfolded protein (Bukau and Horwich, 1998). HSP60 is a major homolog of bacterial GroEL (Zeilstra-Ryalls et al., 1991). This protein is synthesized in the cytosol and imported into mitochondria where it functions as chaperone protein (Singh et al., 1990). HSP60 is also involved in multiple other functions including pro-apoptotic functions and cell signaling (Henderson et al., 2013). Some viral proteins, such as hepatitis B virus (HBV) X protein, interact with HSP60 to induce apoptosis (Tanaka et al., 2004).

Mitochondria play a pivotal role in supplying energy and regulating apoptotic cell death processes. Herpes simplex virus-1^{-1} (HSV-1) infection has been associated with deregulation of mitochondrial function. During HSV-1 infection mitochondrial protein synthesis is progressively reduced (Latchman, 1988; Lund and Ziola, 1986). HSV-1 infection also induces mitochondrial membrane disruption (Tsurumi and Lehman, 1990). Murata et al. demonstrated that mitochondria migrate to the perinuclear region with the tegument proteins U_L41 and U_L46 during HSV-1 infection (Murata et al., 2000). The tegument protein UL16 also contains a mitochondrial localization signal and interacts with mitochondria (Chadha et al., 2017). Likewise, BoHV-1 infection induces mitochondrial dysfunction and is associated with stimulation of apoptosis (Devireddy and Jones, 1999; Xu et al., 2012). Moreover, BoHV-1 infection leads to mitochondrial dysfunction through induction of reactive oxygen species (Zhu et al., 2016). Since several viral proteins targeted to mitochondria are meant to subvert host defenses (reviewed in (Castanier and Arnoult, 2011)), the de-regulation of mitochondrial functions by tegument proteins might be correlated to the establishment of virus infection.

VP8 performs several of its functions through interactions with viral or cellular proteins. Alpha-helical structures often mediate protein-protein interactions (Watkins et al., 2015). The C-terminal domain of VP8 contains mostly α-helical structures and is responsible for these interactions (Afroz et al., 2016). While expressing and purifying an N-terminally truncated VP8 for structural analysis in *Escherichia coli (E. coli)*, we observed a strongly interacting protein that was co-purified with VP8. By mass spectrometry this bacterial protein was identified as GroEL, which shows conserved homology with mammalian heat shock protein-60 (HSP60). HSP60 is a molecular chaperone located in the cytoplasm and mitochondria and implicated in correct folding and transport of proteins to the mitochondrial matrix. We demonstrated that VP8 interacts with HSP60 in both VP8-transfected and BoHV-1-infected cells. Furthermore, VP8 was localized to mitochondria and caused deregulation of mitochondrial functions.

2. Materials and methods

2.1. Cells, viruses and plasmids

Madin-Darby bovine kidney (MDBK) and HeLa cells were maintained in Eagle's minimum essential medium (MEM, Sigma-Aldrich Canada Ltd, Oakville, ON, Canada) supplemented with 10% heat-inactivated fetal bovine serum (FBS, Gibco, Life Technologies, Burlington, ON, Canada), 10 mM HEPES buffer (Life Technologies) and 1% antibiotic-antimycotic (Life Technologies). A 37 °C incubator with 5% CO_2 was used to culture the cells. BoHV-1, BoHV1-ΔU_L47 and BoHV-1U_L47R were generated previously, (Lobanov et al., 2010) and were propagated in MDBK cells. The plasmid pFLAG-VP8, which allows expression of VP8 with a N-terminal FLAG tag from a cytomegalovirus (CMV) promoter (Labiuk et al., 2009) and pFLAG-EYFP (enhanced yellow fluorescent protein) (Afroz et al., 2016) were both described previously. The bacterial expression vector pET His6 Sumo TEV LIC was a gift from Scott Gradia (Addgene plasmid # 29659). A HSP60 expression plasmid was obtained from Sino Biologicals Inc., Wayne, PA, USA.

2.2. Antibodies and other reagents

BoHV-1 VP8-specific murine monoclonal antibody was raised and used as previously described (van Drunen Littel-van den Hurk et al., 1995). HSP60-specific rabbit polyclonal antibody was obtained from Cell Signaling Technology (Beverly, MA, USA. Murine monoclonal anti-FLAG antibody was purchased from Sigma-Aldrich Canada Ltd, (Oakville, ON, Canada). Anti-cytochrome C antibody was obtained from Abcam (Cambridge, MA, USA). A mitochondria detection kit, MITO-ID Red detection kit, was obtained from Enzo Life Sciences, Inc. (Farmingdale, NY, USA). ATPlite 1step Luminescence Assay system was purchased from PerkinElmer (Waltham, MA, USA).

2.3. Expression and purification of truncated VP8

A truncated ORF of VP8 (amino acids 219–741) was PCR amplified using the primers, GAGGGATCCGAGCGGCTGTCGGAAGGGCCCCCGC TCCTCAAC and CACCTCGAGCTACCGGCCGCCCAGGCGCGGGCCCCG CCCATC, and then cut with BamHI and XhoI and cloned into a modified version of pET His6 Sumo TEV LIC. This allowed for expression of truncated VP8 with an N-terminal SUMO and His tag. A N-terminal SUMO has been shown to enhance expression and solubility of proteins (Marblestone et al., 2006); previous attempts to express VP8 in *E. coli* without SUMO were unsuccessful (results not shown). A Tobacco Etch Virus (TEV) protease site between the SUMO-his and VP8 allowed for removal of the N-terminal tag from the purified protein. Recombinant protein was expressed in transformed BL21 (DE3) competent *E. coli* cells by inducing mid-log phase cells with Isopropyl β-D-1-thiogalactopyranoside (IPTG) at a final concentration of 250 mM and further incubation at 37 °C for 5 h. The cells were harvested by centrifugation at 10,000 x g for 15 min. and resuspended in 20 mM imidazole, 200 mM sodium phosphate buffer, supplemented with a SIGMA*FAST* Protease Inhibitor Cocktail tablet. The cells were lysed with a cell disruptor (Constant system, LTD. USA) and purified with a GE Healthcare His-Trap column. The purified protein was digested with Ac-TEV protease to cleave SUMO-His from the truncated VP8 and was re-purified on the Nickel column. The pure truncated VP8 was concentrated with an Amicon concentrator. Proteins were analyzed by SDS-PAGE followed by Coomassie Brilliant Blue staining and destaining.

2.4. Mass spectrometry

SUMO- and His-tagged truncated VP8 expressed in *E.coli* was purified by using a Nickel column. The purified protein was analyzed by SDS-PAGE and stained with Coomassie Brilliant Blue in 10% acetic acid, 40% methanol. After destaining the gel, the proteins bands were excised and treated for in-gel trypsin digestion. The protein samples were then analyzed using matrix-assisted laser desorption/ionization time-of-flight mass spectrometry (MALDI-TOF-MS) in the Alberta Proteomics and Mass Spectrometry Facility, University of Alberta, Edmonton, Canada. Briefly, the excised protein bands were destained (100 mM ammonium bicarbonate/acetonitrile (50:50)); reduced

(10 mm BME in 100 mm bicarbonate), alkylated (55 mM iodoacetamide in 100 mm bicarbonate) and dehydrated. The dehydrated samples were trypsinized with 6 ng/μl trypsin (Promega Sequencing grade) overnight at room temperature (RT). The tryptic peptides were extracted with 97% water/2% acetonitrile/1% formic acid. The second extraction was performed using 50% of the first extraction buffer and 50% acetonitrile. Nanoflow HPLC (Easy-nLC II, Thermo Scientific) coupled to a LTQ XL-Orbitrap hybrid mass spectrometer (Thermo Scientific) was used to resolve the tryptic peptide fractions. The peptide mixtures were injected onto the column, and the mass spectrometer data were obtained. The data processing was performed with Proteome Discoverer 1.4 (Thermo Scientific) and UniProt (uniprot.org) bovine, *E. coli* and VP8 databases. The data were searched with SEQUEST (Thermo Scientific).

2.5. Cell lysates, immunoprecipitation, and Western blotting

HeLa cells were seeded one day before transfection and grown to 60–70% confluency. The cells were transfected with different plasmids with Lipofectamine and Plus reagents (Invitrogen, Life Technologies). At 24 h post transfection ice-cold phosphate-buffered saline (PSB, pH 7.4) was used to wash the cells followed by incubation with lysis buffer (50 mM Tris, 150 mM NaCl, 1 mM EDTA, 1% Triton X-100, pH 7.4) supplemented with mammalian cell and tissue extract protease inhibitor cocktail (Sigma-Aldrich). The cell and lysis buffer mixture was incubated on ice for 30 min followed by centrifugation at 12,000 × *g* for 15 min at 4 °C. The cell lysates were collected and stored at −80 °C for future use. MDBK cells were infected with BoHV-1 and mutant viruses, and cell lysates were generated and collected as described above.

For immunoprecipitation, the cell lysates were incubated with anti-FLAG resin overnight. Alternatively, the cell lysates were incubated with anti-HSP60 antibody overnight followed by incubation with G-Sepharose Fast Flow beads (GE HealthCare, Niskayuna, NY, USA). The protein complexes were washed, and the bound proteins were eluted by adding SDS-PAGE sample buffer followed by boiling. The protein samples were separated on 10% or 8–16% gradient gels, and then transferred to a nitrocellulose membrane followed by incubation with blocking buffer (5% skim milk in PBS containing Tween-20). The membrane was incubated with an appropriate primary antibody followed by incubation with IRDye680−COonjugated anti-mouse IgG or IRDye-800CW−COonjugated anti-rabbit IgG (LI−COR Bioscience, Lincoln, NE, USA). The images were detected with an Odyssey Infrared Imaging system (LI−COR Bioscience).

2.6. Immunofluorescence

HeLa or MDBK cells were seeded in two-chamber Permanox slides (Lab-Tek, Naperville, IL, USA) in MEM supplemented with 5% FBS. Lipofectamine and Plus reagents were used for mock transfection or transfection with pFLAG-VP8. At 24 h post transfection cells were fixed with 4% paraformaldehyde followed by permeabilization with 0.1% Triton X-100. The cells were blocked with 1% goat serum in PBS. Subsequently, the cells were incubated with primary antibodies for 2 h at RT. MDBK cells were mock-infected or infected with BoHV-1. At 2–24 h post infection the cells were fixed, permeabilized and incubated with primary antibodies. Following subsequent washes, the cells were incubated with Alexa Fluor 488 goat anti-mouse IgG or Alexa Fluor 633 goat anti-rabbit IgG (diluted 1:500; Invitrogen, Life Technologies). The nuclei were incubated with 4′,6-diamino-2-phenylindole (DAPI) containing mounting medium. Mitochondria were detected with a MITO-ID red detection kit (Farmingdale, NY, USA). The cells were treated with MITO-ID red dye according to the manufacturer's instruction. Green laser excitation at 488 nm (Alexa 488), red laser excitation at 633 nm (Alexa 633), and 461 nm for DAPI were used to analyze the confocal images. A Leica SP5 confocal microscope (Leica Microsystems Inc., Concord, ON, Canada) was used to obtain immunofluorescence images. Pearson's correlation coefficients were determined by using Coloc2 software in ImageJ.

2.7. RNA interference

HeLa cells were seeded in 6-well plates one day before transfection with control and HSP60 siRNA containing a pool of 4 individual siRNAs targeting HSP60 (SMART-pool ON-TARGETplus HSP60 siRNA, catalogue no: L-010600-00-0005, Dharmacon, USA). At 24 h post transfection cells were transfected again with HSP60 siRNA together with pFLAG-VP8. At 48 h post transfection with HSP60 siRNA and 24 h post transfection with pFLAG-VP8, the cells were lysed and collected. The protein concentration was measured, and 50 μg of each protein sample were analyzed by Western blotting.

2.8. Measurement of cellular ATP levels

The cellular ATP level was determined with an ATPlite 1step Luminescence assay system (PerkinElmer, Waltham, MA, USA). HeLa cells were cultured in 96-well plates and mock-transfected or transfected with pFLAG or pFLAG-VP8. At 48 h post transfection, the ATP level was measured according to the manufacturer's instructions. Briefly, the ATPlite substrate was added to the wells followed by incubation for 5 min at RT with shaking. Luciferase signals emitting at 560 nm were detected with a VICTOR X light luminescence plate reader (PerkinElmer). The ATP concentration was determined from the standard curve. MDBK cells were mock-infected or infected with BoHV-1, BoHV1-ΔU_L47 or BoHV1-U_L47R. At 24 h post-infection the ATP level was detected as described above.

2.9. Mitochondrial membrane potential detection

A NIR mitochondrial membrane potential kit (Sigma-Aldrich) was used to detect mitochondrial membrane potential (MMP). HeLa cells were mock-transfected or transfected with pFLAG or pFLAG-VP8. At 48 h post-transfection cells were stained with the cationic membrane potential dye according to the manufacturer's instructions. MDBK cells were mock-infected or infected with BoHV-1, BoHV1-ΔU_L47 or BoHV1-U_L47R. At 2, 4 or 24 h post infection the cells were trypsinized and processed to examine the mitochondrial membrane potential. Briefly, mitochondrial membrane potential dye, Near Infrared (NIR), was added to trypsinized cells followed by incubation for 15–30 min. After subsequent washes, the cells were resuspended in assay buffer and were analyzed by fluorescence activated cell sorting (FACS). Fluorescence intensity was monitored with a flow cytometer equipped with a 635 nm red diode laser and a 661 nm filter.

3. Results

3.1. Identification of HSP60 as an interacting partner of BoHV-1 VP8

BoHV-1 VP8 consists of 741 amino acids. Since the C-terminal domain of VP8 is enriched with alpha-helices (Afroz et al., 2016), we expressed this portion of VP8 (amino acids 219–741) in *E. coli* with N-terminal SUMO and His tags. SUMO-His-VP8 219–741 was purified by Nickel affinity chromatography. As shown in Fig. 1A, VP8 with an apparent molecular weight of 75 kDa co-purified with a 60 kDa bacterial protein. Some other minor contaminating proteins were also present with VP8 after the first round of purification. After cleavage of SUMO-His with Ac-TEV protease, we observed nearly complete digestion, which resulted in 52 kDa VP8 and 25 kDa SUMO-His. However, the bacterial protein of 60 kDa remained present even after an additional round of Nickel affinity purification (Fig. 1A right panel); that the 60 kDa protein was not a truncated form of VP8 was confirmed by Western blotting (Fig. 1B). Polyclonal VP8-specific antibody recognized the 52 kDa VP8, but not the 60 kDa protein. This suggested that VP8

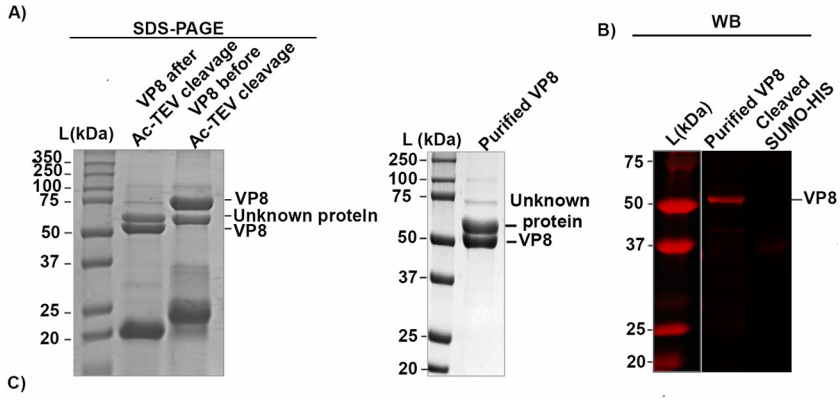

C)

Sample protein	Accession No	Identified protien	Description	Score
Unknown protein – before TEV digestion	Q1R3B6	GroEL, (HSP60Hu)	60kDa chaoeronin OS=E.coli	653
Unknown protein – after final purification	Q1R3B6	GroEL, (HSP60Hu)	60kDa chaoeronin OS=E.coli	5918.24

D)

```
Bacterial GroEL    1 ----------------------MAAKDVKFGNDARVKMLRGVNVLADAVKVTLGPKGR  36
Bovine HSP60       1 MLRLPAVLRQMRPVSRALALHLTRAYAKDVKFGADARALMLQGVDLLADAVAVTMGPKGR  60
Human HSP60        1 MLRLPTVFRQMRPVSRVLAPHLTRAYAKDVKFGADARALMLQGVDLLADAVAVTMGPKGR  60
                                    ******* ***. **:**::***** **:*****

Bacterial GroEL   37 NVVLDKSFGAPTITKDGVSVAREIELEDKFENMGAQMVKEVASKANDAAGDGTTTATVLA  96
Bovine HSP60      61 TVIIEQSWGSPRVTKDGVTVAKSIDLKDKYKNIGAKLVQDVANNTNEEAGDGTTTATVLA 120
Human HSP60       61 TVIIEQSWGSPKVTKDGVTVAKSIDLKDKYKNIGAKLVQDVANNTNEEAGDGTTTATVLA 120
                     .*::::*:*:* :*****:**:.*:*:**::*:**::*::**.::*: ************

Bacterial GroEL   97 QAIITEGLKAVAAGMNPMDLKRGIDKAVTAAVEELKALSVPCSDSKAIAQVGTISANSDE 156
Bovine HSP60     121 RSIAKEGFEKISKGANPVEIRRGVMLAVDAVIVELKKQSKPVTTPEEIAQVATISANGDK 180
Human HSP60      121 RSIAKEGFEKISKGANPVEIRRGVMLAVDAVIAELKKQSKPVTTPEEIAQVATISANGDK 180
                     ::* .**:: :: * **::::**:  ** *.: ***  * * :  : ****.*****.*:

Bacterial GroEL  157 TVGKLIAEAMDKVGKEGVITVEDGTGLQDELDVVEGMQFDRGYLSPYFINKPETGAVELE 216
Bovine HSP60     181 EIGNIISDAMKKVGRKGVITVKDGKTLNDELEIIEGMKFDRGYISPYFINTSKGQKCEFQ 240
Human HSP60      181 EIGNIISDAMKKVGRKGVITVKDGKTLNDELEIIEGMKFDRGYISPYFINTSKGQKCEFQ 240
                      :*::*::**.***:*****:**. *:***:::***:*****:******. :    *::

Bacterial GroEL  217 SPFILLADKKISNIREMLPVLEAVAKAGKPLLIIAEDVEGEALATLVVNTMRGIVKVAAV 276
Bovine HSP60     241 DAYVLLSEKKISSVQSIVPALEIANAHRKPLVIIAEDVDGEALSTLVLNRLKVGLQVVAV 300
Human HSP60      241 DAYVLLSEKKISSIQSIVPALEIANAHRKPLVIIAEDVDGEALSTLVLNRLKVGLQVVAV 300
                     . ::**::****.::.::*.** .     ***:******:****:***:* ::  ::*.**

Bacterial GroEL  277 KAPGFGDRRKAMLQDIATLTGGTVISE-EIGMELEKATLEDLGQAKRVVINKDTTTIIDG 335
Bovine HSP60     301 KAPGFGDNRKNQLKDMAIATGGAVFGEEGLNLNLEDVQPHDLGKVGEVIVTKDDAMLLKG 360
Human HSP60      301 KAPGFGDNRKNQLKDMAIATGGAVFGEEGLTLNLEDVQPHDLGKVGEVIVTKDDAMLLKG 360
                     *******.**  *:*:*  ***:*:.*  : ::**..  .***:. .*::.** : ::.*

Bacterial GroEL  336 VGEEAAIQGRVAQIRQQIEEATSDYDREKLQERVAKLAGGVAVIKVGAATEVEMKEKKAR 395
Bovine HSP60     361 KGDKAQIEKRIQEIIEQLDITTSEYEKEKLNERLAKLSDGVAVLKVGGTSDVEVNEKKDR 420
Human HSP60      361 KGDKAQIEKRIQEIIEQLDVTTSEYEKEKLNERLAKLSDGVAVLKVGGTSDVEVNEKKDR 420
                     *::* *: *: :* :*:: :**:*::****:**:***:.****:***.:::**::*** *

Bacterial GroEL  396 VEDALHATRAAVEEGVVAGGGVALIRVASKLADLRGQNEDQNVGIKVALRAMEAPLRQIV 455
Bovine HSP60     421 VTDALNATRAAVEEGIVLGGGCALLRCIPALESITPANEDQKTGIEIIKKTLKIPAMTIA 480
Human HSP60      421 VTDALNATRAAVEEGIVLGGGCALLRCIPALDSLTPANEDQKIGIEIIKRTLKIPAMTIA 480
                     * ***:*********:* **. **:*    * .:    ****: **::  :::: *   *.

Bacterial GroEL  456 LNCGEEPSVVANTVKGGDGNYGYNAATEEYGNMIDMGILDPTKVTRSALQYAASVAGLMI 515
Bovine HSP60     481 KNAGVEGSLIVEKIMQSSSEVGYDAMLGDFVNMVEKGIIDPTKVVRTALLDAAGVASLLT 540
Human HSP60      481 KNAGVEGSLIVEKIMQSSSEVGYDAMAGDFVNMVEKGIIDPTKVVRTALLDAAGVASLLT 540
                      *.* * *::.:.:  ...: **:*   :: **:: **:*****.*:**  **.**.*:

Bacterial GroEL  516 TTECMVTDLPKNDAADLGAAGGMGGMGGMM----- 548
Bovine HSP60     541 TAEVVVTEIPKEEKD-----PGMGGMGGMGGGMGGGMF 573
Human HSP60      541 TAEVVVTEIPKEEKD-----PGMGAMGGMGGGMGGGMF 573
                     *:* :**::**::        ***.****** *
```

Fig. 1. Identification of a bacterial protein co-purified with recombinant VP8. A) SUMO-His-VP8 219–741 was expressed in BL21 cells. Nickel column-purified VP8 was digested with Ac-TEV protease and analyzed by SDS-PAGE followed by Coomassie Brilliant Blue staining. In the right panel of A) purified VP8 was analyzed by SDS-PAGE B) Final purified VP8 and purified SUMO-His were analyzed by Western blotting. L represents protein molecular weight ladder in kDa. C) Purified VP8 was analyzed by SDS-PAGE followed by Coomassie Brilliant Blue staining. The upper 60 kDa protein band (from Fig. 1 A, right panel) was excised and analyzed by MALDI-TOF-MS. The identified peptides were used to search Uniprot data bases and the sum of the score of peptides is presented in the table. D) Sequence homology between bacterial GroEL and bovine and human HSP60 was analyzed by ClustalW. The gray boxes represent homologous sequences. The number indicates amino acid position. A * (asterisk) indicates the position of a single, fully conserved residue. Conservation between groups of strongly similar properties is indicated by a colon (:). A period (.) represents conservation between groups of weakly similar properties.

was strongly associated with a bacterial protein, which consistently co-purified with VP8.

The identity of the co-purified 60 kDa protein was determined by mass spectrometry of the protein bands excised from the gels before TEV digestion and after final purification; in both cases the mass spectrometry analysis showed high MASCOT scores with *E. coli* GroEL (Fig. 1C). GroEL, a 60 kDa chaperonin protein, is required to maintain proper folding of many proteins. Alignment analysis (Fig. 1D) demonstrated considerable sequence similarity between bacterial GroEL and bovine and human HSP60. The identity between bacterial GroEL and human HSP60 is more than 50% (Zhang et al., 2005), while the homology between human and bovine is 98%. The bacterial GroEL lacks the N-terminal sequences that are responsible for targeting HSP60 to mitochondria in bovine and human cells. The fortuitous observation that recombinant VP8 strongly associated with bacterial GroEL led to the hypothesis that VP8 interacts with host HSP60 during viral infection contributing to virulence; the HSP60 may serve to stabilize VP8 or translocate VP8 to the mitochondria leading to impairment of mitochondrial function.

3.2. Interaction of BoHV-1 VP8 with mammalian HSP60

Interaction between HSP60 and VP8 was determined by immunoprecipitation following transfection of HeLa cells with plasmid

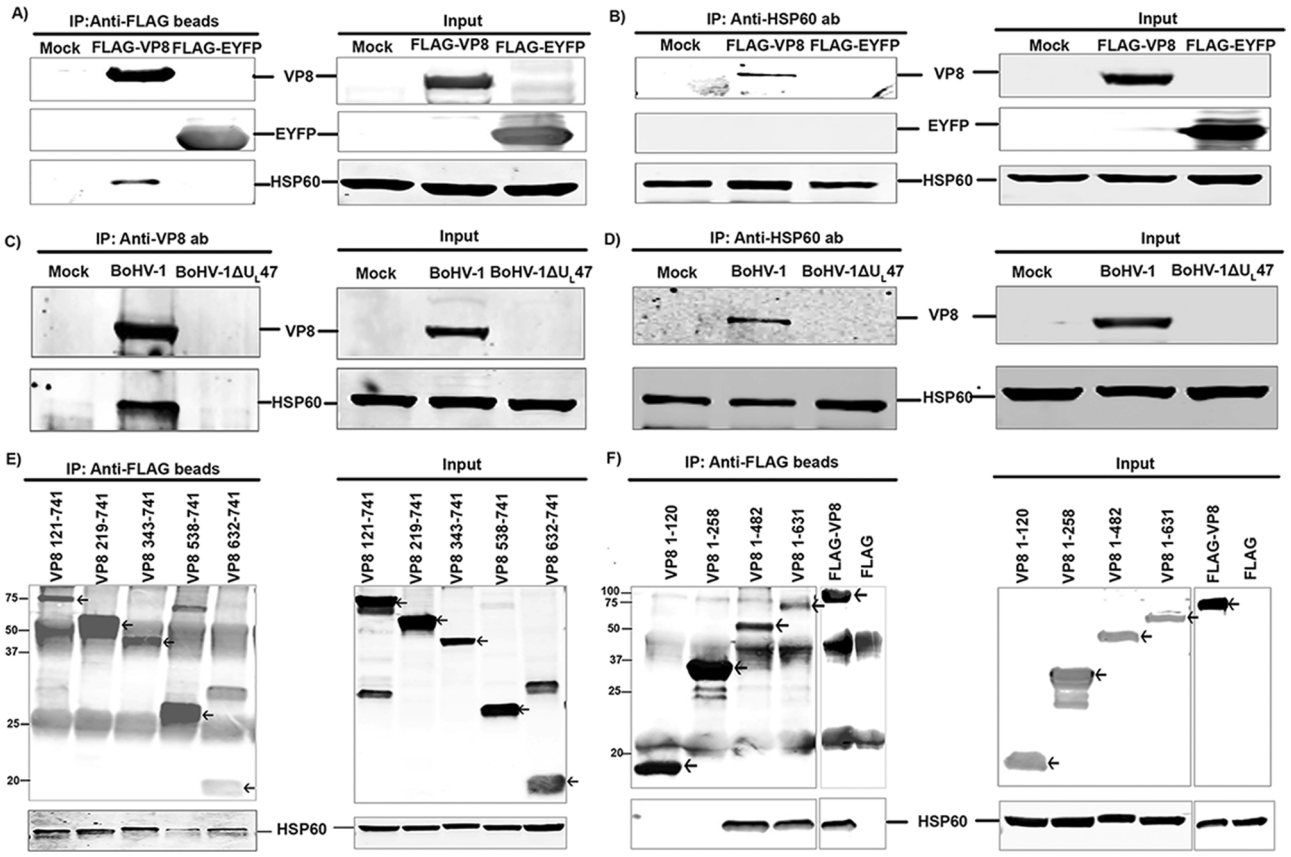

Fig. 2. Interaction of BoHV-1 VP8 with HSP60 in eukaryotic cells. A) HeLa cells were mock-transfected or transfected with pFLAG-EYFP or pFLAG-VP8. Cell lysates were collected at 24 h post transfection and incubated with anti-FLAG beads. B) HeLa cells were mock-transfected or transfected with pFLAG-EYFP or pFLAG-VP8. Cell lysates were collected at 24 h post transfection and incubated with rabbit anti-HSP60 antibody, followed by with G Sepharose Fast Flow beads. In A) and B) precipitated proteins (left panel) and input lysates (right panel) were detected with anti-FLAG and anti-HSP60 antibodies. C) MDBK cells were mock-infected or infected with BoHV-1 or BoHV-1ΔU_L47 at a MOI of 3, and at 24 h post infection cell lysates were collected and incubated with mouse anti-VP8 antibody followed by G Sepharose Fast Flow beads. D) MDBK cells were mock-infected or infected with BoHV-1 or BoHV-1ΔU_L47 as described above. At 24 h post infection cell lysates were collected and incubated with anti-HSP60 antibody followed by G Sepharose Fast Flow beads. In C) and D) precipitated proteins (left panel) and input lysates (right panel) were detected with anti-VP8 and anti-HSP60 antibodies. E) HeLa cells were mock-transfected or transfected with five N-terminally truncated VP8 versions. Cell lysates were collected at 24 h post transfection and incubated with anti-FLAG beads. F) HeLa cells were mock-transfected or transfected with pFLAG or pFLAG-VP8 or four different C-terminally truncated VP8 versions. Cell lysates were collected at 24 h post transfection and incubated with anti-FLAG beads. In E) and F) precipitated proteins (left panel) and input lysates (right panel) were detected with anti-FLAG and anti-HSP60 antibodies.

expressing FLAG-tagged VP8. Since the transfection efficiency of MDBK cells is very low (1.7-2.4%) (Osorio and Bionaz, 2017), HeLa cells were used for transfection assays. At 24 h post transfection, cell lysates were collected. Anti-FLAG resin precipitated VP8 and EYFP from VP8- and EYFP-transfected cells, respectively, whereas HSP60 was precipitated with FLAG-VP8, but not with FLAG-EYFP (Fig. 2A). Similarly, mock-, pFLAG- and pFLAG-VP8-transfected cell lysates were analyzed by reverse immunoprecipitation with an anti-HSP60 antibody (Fig. 2B), which precipitated HSP60 from mock-, FLAG- and FLAG-VP8-transfected cells, as expected. However, anti-HSP60 antibody precipitated only FLAG-VP8, and not FLAG-EYFP, confirming interaction of VP8 with HSP60.

To demonstrate interaction of VP8 with HSP60 in BoHV-1-infected cells, MDBK cells were mock-infected or infected with BoHV-1 or BoHV-1ΔU_L47. At 24 h post infection cell lysates were collected and incubated with a VP8-specific antibody followed by G-Sepharose Fast Flow beads (Fig. 2C). The VP8-specific antibody precipitated VP8 from BoHV-1-infected cells, but not from mock- or BoHV-1ΔU_L47-infected cells. The precipitated VP8 pulled down HSP60 from BoHV-1-infected cells, but not from mock- or BoHV-1ΔU_L47-infected cells, thus demonstrating that VP8 interacts with HSP60 during BoHV-1 infection. This was validated by reverse precipitation of VP8; mock-, BoHV-1- and BoHV-1ΔU_L47-infected cell lysates were incubated with an anti-HSP60 antibody followed by G-Sepharose Fast Flow beads (Fig. 2D). HSP60-specific antibody pulled down HSP60 from mock-, BoHV-1- and BoHV-1ΔU_L47-infected cell lysates, while VP8 was precipitated only from BoHV-1-infected cells. This confirms that HSP60 interacts with VP8 in BoHV-1-infected cells. Altogether, these experiments demonstrate interaction of VP8 with HSP60 in both VP8-transfected and BoHV-1-infected cells.

To determine the domain of VP8 interacting with HSP60, five different FLAG-tagged, N-terminally truncated VP8 versions (VP8 121–741, VP8 219–741, VP8 343–741, VP8 538–741, and VP8 632–741) were analyzed for precipitation of HSP60 (Fig. 2E). Anti-FLAG resin pulled down all N-terminally truncated VP8 versions and HSP60 indicating that a region between amino acids 632–741 of VP8 is sufficient for interaction with HSP60. In addition, cells were transfected with C-terminally truncated VP8 versions (VP8 1–120, VP8 1–258, VP8 1–482, VP8 1–631) and incubated with anti-FLAG resin. Only two C-terminally truncated VP8 versions (VP8 1–482 and VP8 1–631) precipitated HSP60. This experiment revealed that when amino acids 259–482 are present, VP8 precipitated HSP60. Collectively, this suggests that regions within amino acids 259–482 and 632–741 of VP8 are involved in binding of VP8 to HSP60.

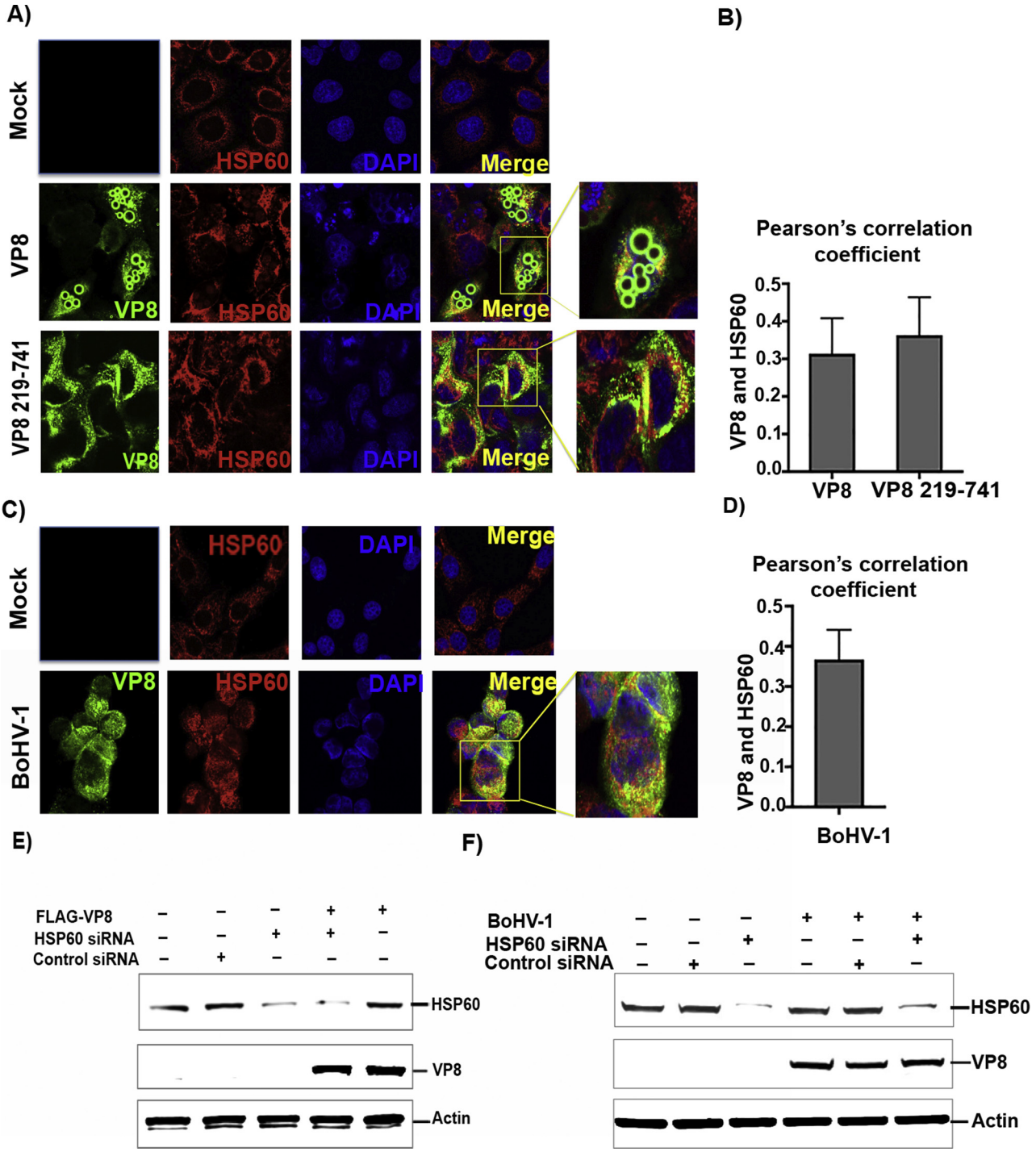

Fig. 3. HSP60 co-localizes with VP8, but does not alter VP8 expression. A) HeLa cells were mock-transfected or transfected with pFLAG-VP8 or pFLAG-VP8 219–741. At 24 h post transfection cells were incubated with mouse anti-FLAG and rabbit anti-HSP60 antibodies followed by incubation with Alexa Fluor 488-conjugated goat anti-mouse and Alexa Fluor 633-conjugated goat anti-rabbit IgG. Nuclei were identified with DAPI. Yellow boxes represent higher magnifications of the selected areas. B) To quantify co-localization of VP8 and HSP60 Pearson's correlation coefficients were determined by using Coloc2 software in ImageJ. Pearson's correlation coefficients of VP8 or VP8 219–741 and HSP60 were calculated from 20 random cells. Data are shown as mean ± SD; C) MDBK cells were infected with BoHV-1 at a MOI of 3 for 14 h. The infected cells were incubated with monoclonal anti-VP8 and polyclonal anti-HSP60 antibodies followed by incubation with Alexa Fluor 488-conjugated goat anti-mouse and Alexa Fluor 633-conjugated goat anti-rabbit IgG. Nuclei were identified with DAPI. The yellow box represents higher magnifications of the selected area. D) To quantify co-localization of VP8 and HSP60 in BoHV-1 infected cells, Pearson's correlation coefficients were determined by using Coloc2 software in ImageJ. Pearson's correlation coefficients of VP8 and mitochondria were calculated from 20 random cells. Data are shown as mean ± SD. E) HeLa cells were mock-transfected or transfected with control siRNA or HSP60 siRNA for 24 h before transfecting again with control siRNA or HSP60 siRNA together with FLAG-VP8 or with only FLAG-VP8. At 24 h post transfection cell lysates were collected, and 50 µg proteins of each sample were analyzed by SDS-PAGE and Western blotting. HSP60, VP8 and actin were detected with anti-HSP60, anti-FLAG and anti-actin antibodies, respectively. F) EBTr cells were mock-transfected or transfected with control siRNA or HSP60 siRNA for 24 h before transfecting again with control siRNA or HSP60 siRNA together with mock-infection or infection with BoHV-1. At 48 h post transfection and 24 post infection cell lysates were collected, and 50 µg protein of each sample was analyzed by SDS-PAGE and Western blotting. HSP60, VP8 and actin were detected with anti-HSP60, anti-VP8 and anti-actin antibodies, respectively.

3.3. HSP60 co-localizes with VP8 but does not alter VP8 expression

Since VP8 interacts with HSP60 in mammalian cells, we investigated whether VP8 co-localizes with HSP60. HeLa cells were mock-transfected or transfected with pFLAG-VP8 or pFLAG-VP8 219–741. At 24 h post transfection cells were incubated with anti-FLAG or anti-HSP60 antibodies. FLAG-VP8 219–741 contains the domains implicated in binding to HSP60, but it lacks a nuclear localization signal. As demonstrated in Fig. 3A, VP8, as well as VP8 219–741, partially co-localized with HSP60. Pearson's correlation coefficient analysis further confirmed co-localization of VP8 and VP8 219–741 with HSP60 (Fig. 3B). To demonstrate co-localization of HSP60 with VP8 in BoHV-1-infected cells, MDBK cells were mock-infected or infected with BoHV-1. At 14 h post infection the cells were incubated with anti-VP8 and anti-HSP60 antibodies. VP8 contains at least two NESs and is exported out of the nucleus and by 14 h post infection VP8 is detected in the cytoplasm (Verhagen et al., 2006; Zheng et al., 2004). As indicated in Fig. 3C, some VP8 was cytoplasmic at 14 h post infection and was co-localized with HSP60 in BoHV-1-infected cells at this time point. Furthermore, Pearson's correlation coefficient analysis also indicated co-localization of VP8 with HSP60 (Fig. 3D). These experiments demonstrate partial co-localization of VP8 with HSP60.

HSP60 is known to regulate the folding and maintain the stability of mitochondria- imported proteins (Lin and Rye, 2006). Since VP8 interacted and co-localized with HSP60, we investigated whether HSP60 was required for VP8 expression. HeLa cells were transfected with control or HSP60-specific siRNA, and 24 h later the cells were again transfected with HSP60-specific siRNA and with pFLAG-VP8. At 24 h after transfection with pFLAG-VP8 cell lysates were collected, and equal amounts of the cell lysates were analyzed by Western blotting. The HSP60 level was similar in mock- and control siRNA-transfected cells (Fig. 3E), but was substantially reduced in cells transfected with HSP60-specific siRNA. However, the level of VP8, as detected by Western blotting, was not notably altered by the silencing of HSP60 suggesting that HSP60 does not play a major role in maintaining VP8 protein levels. Next, we investigated whether HSP60 functions to maintain VP8 expression during BoHV-1 infection. Since we had to transfect cells with HSP60 siRNA, we used embryonic bovine tracheal cells (EBTr) cells which can be readily transfected (Vassilev et al., 1997) and infected with BoHV-1. While Madin-Darby bovine kidney (MDBK) cells are widely used for BoHV-1 infection, the transfection efficiency in MDBK cells is very low, approximately 1.7%–2.4 % (Osorio and Bionaz, 2017). EBTr cells were transfected with control or HSP60-specific siRNA. At 24 h post transfection the cells were again transfected with control or HSP60-specific siRNA and were either mock-infected or infected with BoHV-1. At 24 h post infection and 48 h post transfection cell lysates were subjected to Western blotting. In mock- and control siRNA-transfected cells HSP60 expression was unchanged. HSP60 expression was notably reduced in HSP60 siRNA-transfected cells (Fig. 3F) compared to mock- and control siRNA-transfected cells. However, the VP8 expression pattern remained unchanged in BoHV-1-infected and HSP60 siRNA-transfected cells, whereas minimal HSP60 was present compared to BoHV-1-infected and control siRNA-transfected cells. This result demonstrates that HSP60 is not required for maintaining VP8 expression during BoHV-1 infection.

3.4. Localization of HSP60 and VP8 to mitochondria

HSP60 is a mitochondrial protein and contains a mitochondrial localization signal (Singh et al., 1990). We confirmed the localization of HSP60 to the mitochondria by incubating HeLa cells with anti-HSP60 antibody and mito-tracker red dye (Fig. 4A). Since VP8 interacts with HSP60, and HSP60 localizes to mitochondria, we anticipated that VP8 might be localized to the mitochondria. HeLa cells were mock-transfected or transfected with pFLAG-VP8 or pFLAG-VP8-219–741. At 24 h post transfection the cells were incubated with anti-FLAG antibody and with mito-tracker red dye. The full-length VP8 and VP8 219–741 were both partially localized to mitochondria, which indicates that like HSP60, VP8 is targeted to the mitochondria and that the C-terminal domain of VP8, VP8 219–741, is sufficient for the mitochondrial localization of VP8 (Fig. 4B). Furthermore, Pearson's correlation coefficient analysis supported co-localization of VP8 and VP8 219–741 with mitochondria (Fig. 4C). VP8 expression appeared to substantially change the mitochondrial matrix. In addition, we identified the mitochondria with anti-cytochrome C antibody. HeLa cells were mock-transfected or transfected with pFLAG-VP8. At 24 h post transfection the cells were incubated with anti-FLAG and anti-cytochrome C antibodies (Fig. 4D), which showed co-localization of VP8 with cytochrome C. This was confirmed by Pearson's correlation coefficient analysis (Fig. 4E).

To investigate localization of VP8 to the mitochondria during BoHV-1 infection, MDBK cells were mock-infected or infected with BoHV-1. At 14 h post infection cells were incubated with anti-VP8 antibody and mito-tracker red dye. As shown in Fig. 4F, VP8 partially localized to mitochondria in BoHV-1-infected cells. Furthermore, Pearson's correlation coefficient analysis also confirmed co-localization of VP8 with mitochondria in BoHV-1 infected cells (Fig. 4G). These experiments confirm partial localization of VP8 to mitochondria in both VP8-transfected and BoHV-1-infected cells.

3.5. Localization of VP8 to mitochondria at different time points during BoHV-1 infection

Since VP8 localized to mitochondria in both VP8-transfected and BoHV-1-infected cells, it was of interest to investigate at which time point this occurs during infection. MDBK cells were mock-infected or infected with BoHV-1, and at different times post infection the cells were fixed and incubated with an anti-VP8 antibody and mito-tracker red dye. As shown in Fig. 5, VP8 was cytoplasmic at 2 h post infection, as previously demonstrated (Afroz et al., 2016; Vasilenko et al., 2012), and some VP8 was localized to the mitochondria at this time. As the infection progressed, at 4 h post infection VP8 was observed in the nucleus, the peri-nuclear region, and the cytoplasm. Some of the peri-nuclear VP8 co-localized with the mitochondria. At 6 h post infection most of VP8 was nuclear, but some peri-nuclear VP8 was localized to the mitochondria. As reported previously VP8 is exported to the cytoplasm later during infection (van Drunen Littel-van den Hurk et al., 1995; Vasilenko et al., 2012). At 14 h post infection, VP8 was localized in the cytoplasm and some VP8 was observed in the mitochondria. This experiment illustrates that VP8 partially localized to mitochondria at different time points throughout BoHV-1 infection.

3.6. Effect of VP8 on mitochondrial function

During HSV-1 and BoHV-1 infection mitochondrial dysfunction is caused by the reduction of the MMP (Murata et al., 2000; Zhu et al., 2016). Since VP8 interacted with HSP60 and localized to the mitochondria, we examined whether VP8 causes mitochondrial dysfunction. To measure the MMP in VP8-transfected cells in the absence of any other viral protein, HeLa cells were mock-transfected or transfected with pFLAG, pFLAG-VP8 or pFLAG-VP8 219–741. At 48 h post transfection the MMP was determined with NIR MMP dye and analyzed by FACS (Fig. 6A). The MMP was reduced from approximately 98% in mock- or pFLAG- transfected cells to about 78% in pFLAG-VP8 or pFLAG-VP8 219–741-transfected cells.

To further determine involvement of the VP8 and HSP60 interaction in reduction of the MMP, we analyzed the cellular MMP in the presence of exogenous HSP60 and VP8. HeLa cells were mock-transfected or transfected with pFLAG, pFLAG-VP8, pFLAG-VP8 219–741 or pFLAG-VP8 1–218 (the domain that does not interact with HSP60) together with empty vector or plasmid encoding HSP60 (Fig. 6B). At 48 h post transfection, cells were incubated with NIR MMP dye, and the MMP was determined by FACS. As demonstrated in Fig. 6B, transfection of

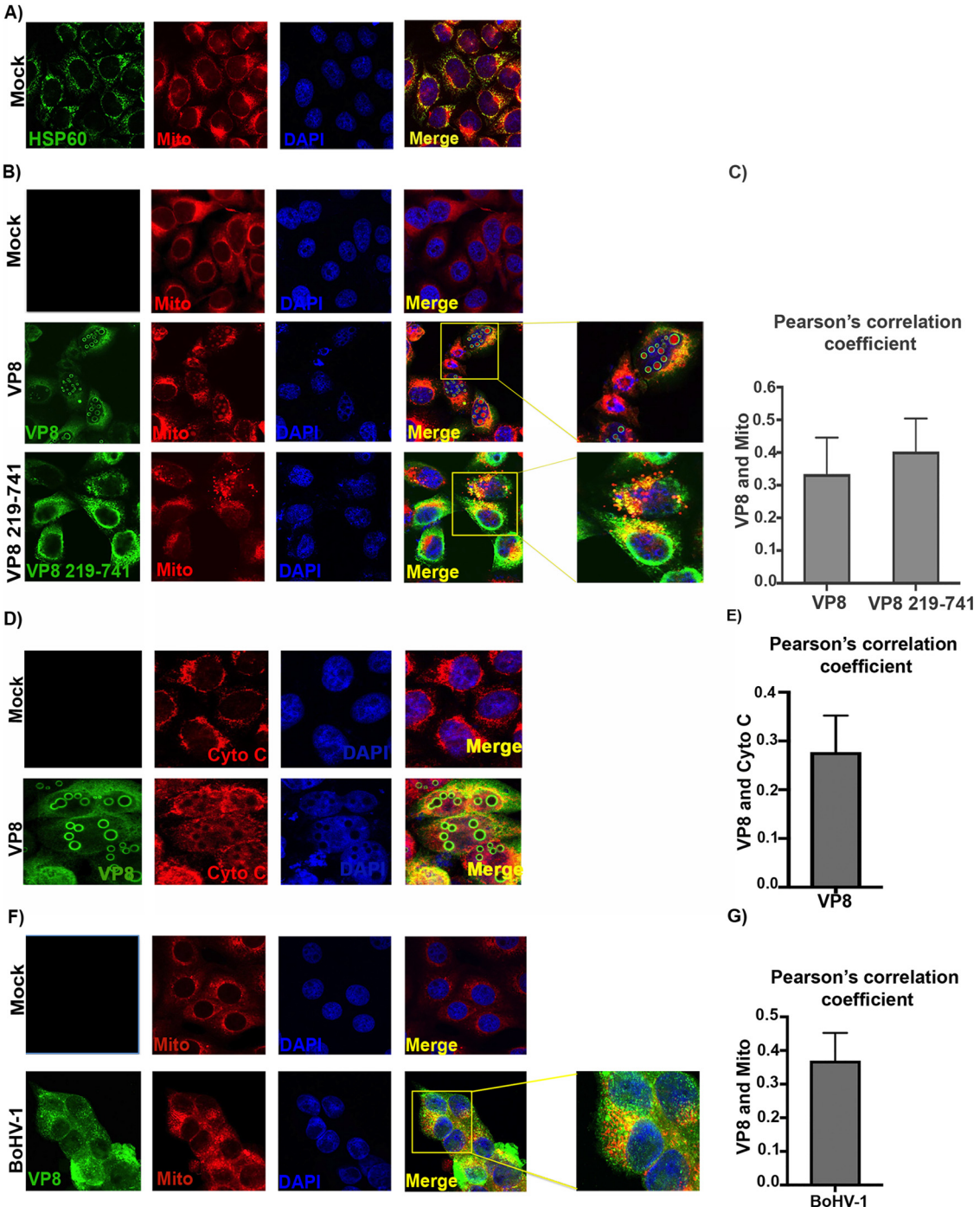

Fig. 4. Localization of HSP60 and VP8 to mitochondria. A) HeLa cells were incubated with polyclonal anti-HSP60 antibody followed by Alexa Fluor 488-conjugated goat anti-mouse IgG. Mitochondria were identified with mitotracker red dye followed by nuclear staining with DAPI. B) HeLa cells were mock-transfected or transfected with pFLAG-VP8 or pFLAG-VP8 219–741. At 24 h post transfection cells were incubated with monoclonal anti-FLAG antibody followed by Alexa Fluor 488-conjugated goat anti-mouse IgG. Mito-tracker red dye was used to identify mitochondria. Nuclei were incubated with DAPI. C) –. Pearson's correlation coefficients for VP8 or VP8 219–741 and mitochondria were calculated from 20 random cells by using Coloc2 software in ImageJ. Data are shown as mean ± SD. D) HeLa cells were mock-transfected or transfected with pFLAG-VP8. At 24 h post transfection cells were incubated with anti-FLAG and anti-cytochrome C antibody followed by Alexa Fluor 488-conjugated goat anti-mouse IgG and Alexa Fluor 633-conjugated goat anti-rabbit IgG. Nuclei were incubated with DAPI. E) The Pearson's correlation coefficient for VP8 and cytochrome C was calculated from 20 random cells as described above. Data are shown as mean ± SD. F) MDBK cells were infected with BoHV-1 at a MOI of 3 for 14 h. The infected cells were incubated with a monoclonal anti-VP8 antibody followed by Alexa Fluor 488-conjugated goat anti-mouse IgG. Mitochondria were incubated with mito-tracker red dye. DAPI was used to identify the nucleus. Yellow boxes represent higher magnifications of selected areas. G) The Pearson's correlation coefficientfor VP8 and mitochondria were calculated from 20 random cells as described above. Data are shown as mean ± SD.

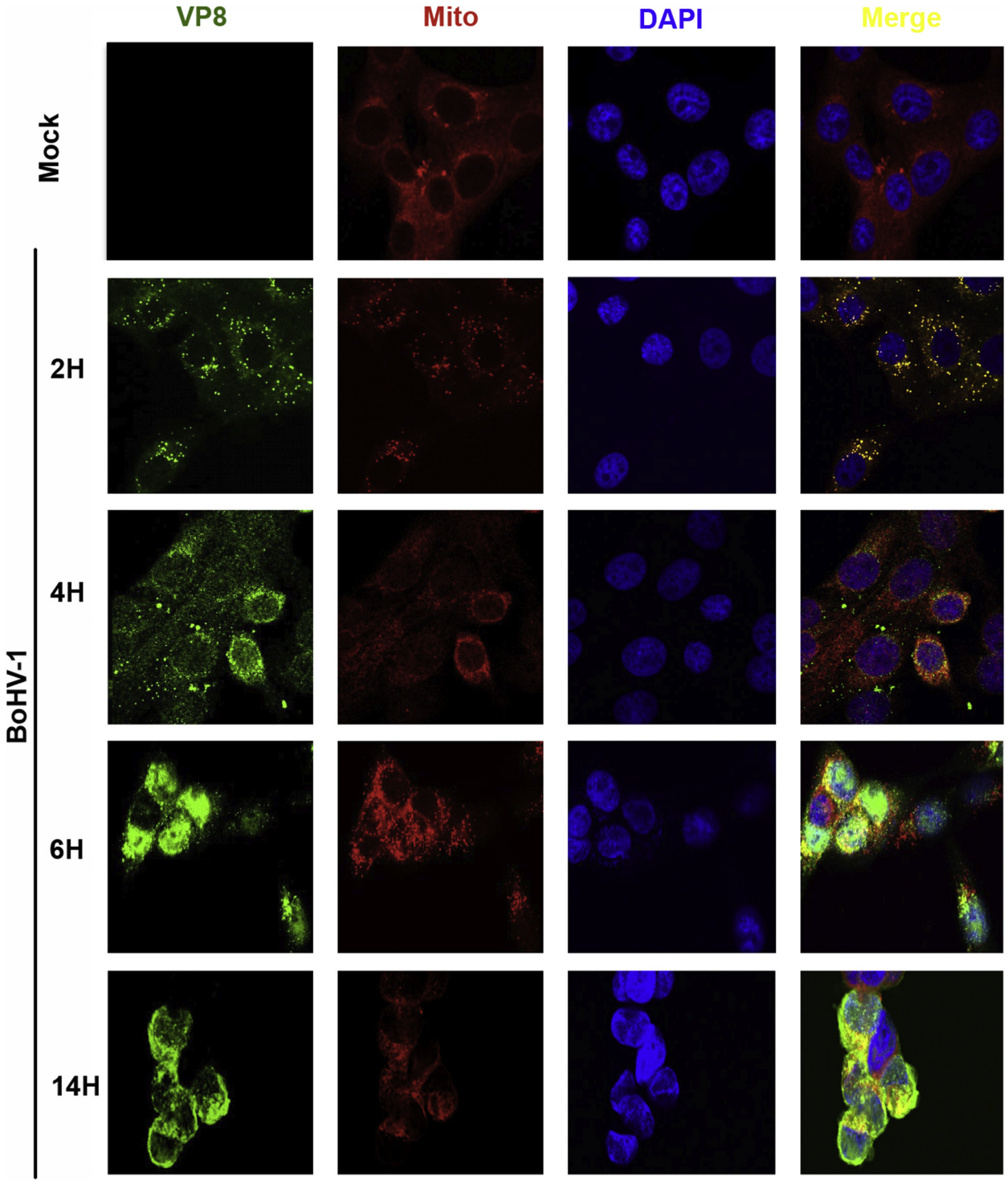

Fig. 5. Localization of VP8 to mitochondria during BoHV-1 infection at different time points. MDBK cells were mock-infected or infected with BoHV-1 at a MOI of 3. Cells were fixed at 2, 4, 6 h or 14 h, and then incubated with a monoclonal anti-VP8 antibody followed by Alexa Fluor 488-conjugated goat anti-mouse IgG. Mitochondria were identified with mito-tracker red dye. DAPI was used to identify the nucleus.

cells with empty vector together with pFLAG-VP8 or pFLAG-VP8 219–741 significantly reduced the MMP (to ~ 68–71%) when compared to mock transfection or transfection with pFLAG together with empty vector (~ 95%). However, in the cells co-transfected with pFLAG-VP8 1–218 and empty vector the MMP was maintained at ~ 91%. In addition, when cells were co-transfected with pFLAG-VP8 or pFLAG-VP8 219–741 and HSP60, the MMP significantly declined (to ~ 49–53%) when compared to cells co-transfected with or pFLAG-VP8 1–218 and plasmid encoding HSP60 (~ 88%). Introduction of HSP60-encoding plasmid and pFLAG did not reduce the MMP. This experiment demonstrates that overexpression of VP8 and HSP60 contributes to the reduction of MMP, and that VP8 219–741 causes reduction of MMP at a similar level as VP8.

Since we observed loss of MMP in VP8-transfected cells, we determined the effect of VP8 on MMP in BoHV-1-infected cells. In this experiment, MDBK cells were mock-infected or infected with BoHV-1,

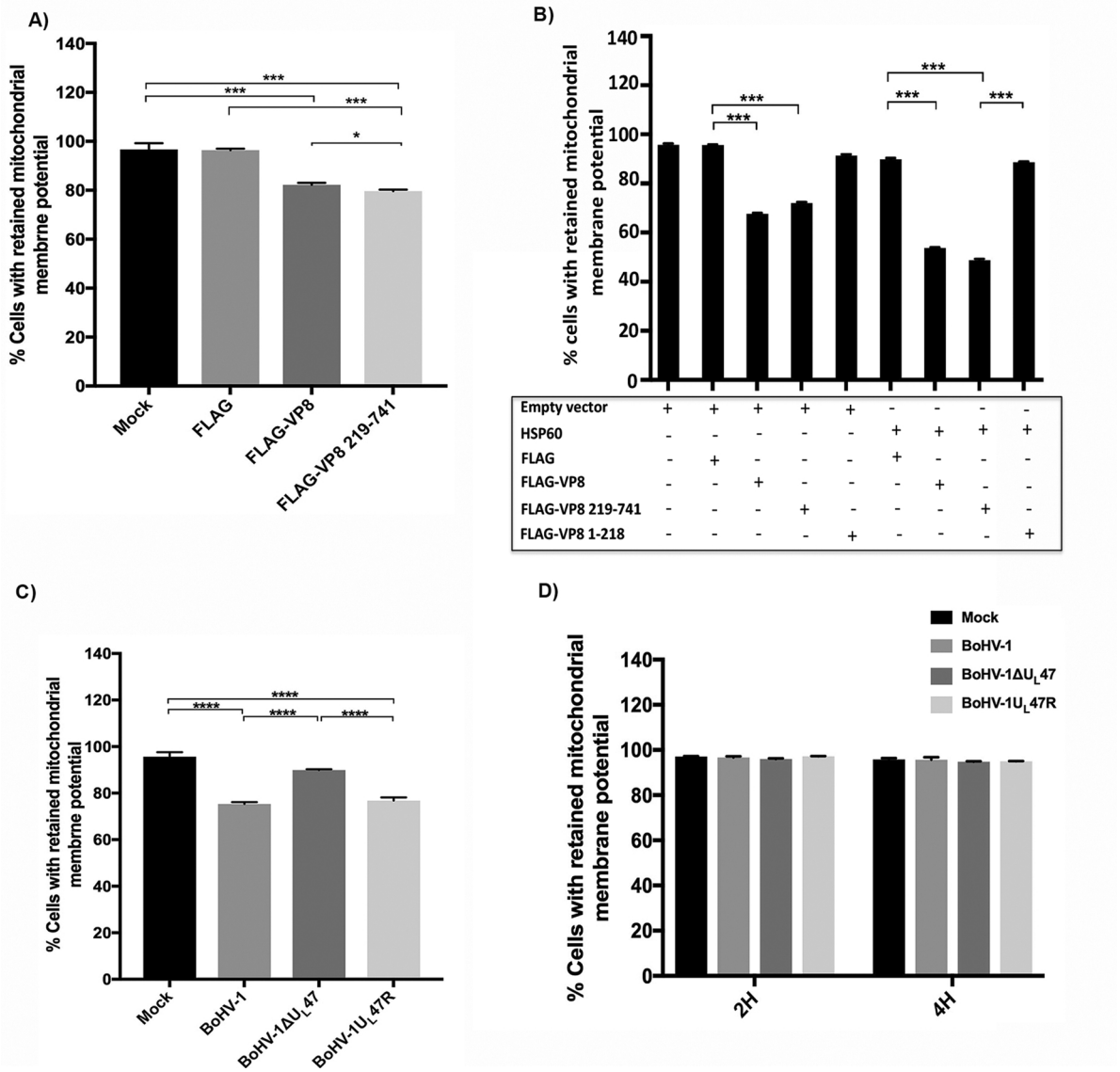

Fig. 6. Effect of VP8 on mitochondrial membrane potential. A) HeLa cells were mock transfected or transfected with pFLAG, pFLAG-EYFP, pFLAG-VP8 or pFLAG-VP8 219–741. At 48 h post transfection cells were trypsinized, incubated with NIR MMP dye and analyzed by FACS. B) Hela cells were transfected with empty vector together with pFLAG, pFLAG-VP8, pFLAG-VP8 219–741, pFLAG-VP8 1–218, or pHSP60, or transfected with pHSP60 together with pFLAG-VP8, pFLAG-VP8 219–741 or pFLAG-VP8 1–218. At 48 h post transfection the cells were trypsinized and then incubated with NIR MMP dye. The cells were analyzed by FACS. C) MDBK cells were mock-infected or infected with BoHV-1, BoHV-1ΔU$_L$47 or BoHV-1U$_L$47R at a MOI of 3 for 24 h. The MMP was detected with the NIR dye and the cells were analyzed by FACS. D) MDBK cells were mock-infected or infected with BoHV-1 at a MOI of 3. At 2 h and 4 h post infection, the cells were trypsinized and then incubated with MMP dye. The cells were analyzed by FACS. The data were analyzed by unpaired *t* test. Statistical significance is indicated by asterisks (****, $P < 0.0001$).

BoHV-1ΔU$_L$47 or BoHV-1U$_L$47R. At 24 h post infection the cells were processed for MMP detection, and were evaluated by FACS. As shown in Fig. 6C, in mock- and BoHV-1ΔU$_L$47-infected cells the MMP was maintained in approximately 90% of the cells, whereas the MMP was retained in approximately 70% of the BoHV-1 and BoHV-1U$_L$47R-infected cells. Thus, BoHV-1 and BoHV-1U$_L$47R infection significantly decrease cellular MMP. Since BoHV-1ΔU$_L$47 infection retained MMP in a higher percentage of cells compared to BoHV-1 and BoHV-1U$_L$47R infection, VP8 can reduce the MMP during BoHV-1 infection.

To determine whether the localization of VP8 to mitochondria at early time points reduces the MMP, we determined the MMP at 2 h and 4 h post infection (Fig. 6D). MDBK cells were mock-infected or infected with BoHV-1, BoHV-1ΔU$_L$47 or BoHV-1U$_L$47R. The cells were collected at 2 h and 4 h post infection and then incubated with NIR MMP dye. The cellular MMP was analyzed by FACS. As indicated in Fig. 6D, the MMP was maintained at these time points of the infection. This experiment demonstrates that the localization of VP8 to mitochondria early during infection does not cause reduction of MMP.

Mitochondria are associated with the energy metabolism by generation of ATP. Proper MMP maintains maximal ATP production. Many viruses modulate mitochondrial function to promote infection. HSV-1, as well as BoHV-1, reduce ATP production during productive infection (Murata et al., 2000; Zhu et al., 2016). Since we observed reduction of MMP in the presence of VP8, we evaluated the total cellular ATP level in VP8-transfected cells. HeLa cells were mock-transfected or transfected with pFLAG, pFLAG-VP8, or pFLAG-VP8 219–741. At 48 h post transfection the total ATP concentration was measured. As demonstrated in Fig. 7A, the total ATP concentration was significantly decreased in VP8- and VP8 219–741 -transfected cells when compared to mock- and FLAG-transfected cells. Thus, this experiment suggests that the presence of VP8 reduced the total ATP level in transfected cells. To determine the effect of VP8 on the total ATP level during BoHV-1

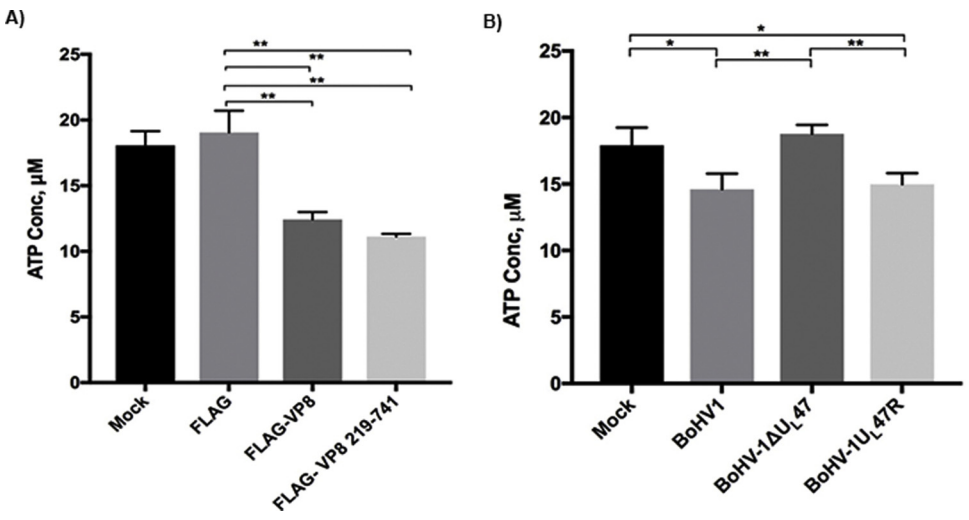

Fig. 7. Reduction of ATP production by BoHV-1 VP8. A) HeLa cells were mock-transfected or transfected with pFLAG, pFLAG-EYFP, pFLAG-VP8 or pFLAG-VP8 219–741. The ATP concentration was determined at 48 h post transfection. B) MDBK cells were mock-infected or infected with BoHV-1, BoHV1-ΔU_L47 or BoHV1-U_L47R at a MOI of 3. ATP concentrations were determined 24 h post infection. The data were analyzed by unpaired *t* test. Statistical significance is indicated by asterisks (*, $P < 0.05$; **, $P < 0.1$).

infection, MDBK cells were mock-infected or infected with BoHV-1, BoHV-1ΔU_L47 or BoHV-1U_L47R. At 24 h post infection, the cellular ATP concentration was evaluated (Fig. 7B). The amount of total ATP was significantly reduced in cells infected with BoHV-1 or BoHV-1U_L47R. However, in BoHV-1ΔU_L47-infected cells the ATP concentration was not affected. Hence, VP8 contributes to the reduction of ATP levels during BoHV-1 infection.

4. Discussion

To obtain purified protein for structural characterization, we expressed the C-terminal domain (amino acids 219–741) of VP8 in *E.coli*. The addition of a SUMO tag, which often enhances production and solubility of recombinant proteins, permitted substantial expression of soluble VP8 in *E. coli*. The recombinant VP8 consistently co-purified with a strongly associated bacterial protein, which was identified as GroEL protein, a homolog of mammalian HSP60, a mitochondrial chaperone protein. VP8 interacted with HSP60 in eukaryotic cells, both after transfection with VP8-expressing plasmids and infection with BoHV-1. Among the three structural domains of GroEL or HSP60, apical, intermediate and equatorial, the equatorial domain contains the most α-helical structures and facilitates interactions with other proteins (Braig et al., 1994). BoHV-1 VP8 might bind to this equatorial domain of HSP60 in a similar manner as other substrates of HSP60. GroEL substrates usually contain two or more domains with α-helices or β-sheets (Houry et al., 1999). According to the predicted secondary structure, the VP8 C-terminal domain is enriched with α-helical structures (Afroz et al., 2016). Immunoprecipitation analysis of different truncated versions of VP8 showed that sequences in its central and C-terminal domain, amino acids 259–482 and 632–741, were involved in interaction with HSP60. Hence, the presence of α-helices at the C-terminus of VP8 might facilitate association of HSP60 and VP8. As HSP60 is a chaperone protein that promotes proper protein folding and stability (Lin and Rye, 2006), we speculated that HSP60 might promote VP8 stability. However, knock down of HSP60 by HSP60-specific siRNA, did not alter VP8 levels suggesting that HSP60 does not play a major role in maintaining the level of VP8 expression.

HSP60 is translated in the cytosol before migrating into the mitochondria (Singh et al., 1990). Consequently, HSP60 is localized both in the cytoplasm and mitochondria (Itoh et al., 2002). In heart and muscle cells around 25–30% of HSP60 has been detected in the cytoplasm, whereas in other cell types this ranges between 15–20% (reviewed in (Gupta and Knowlton, 2005)). The localization of HSP60 in various cellular compartments implies different functions (Henderson et al., 2013), including correct protein folding, cell signaling, maturation and activation of pro-caspase-3 in the cytosol, and activation of nuclear factor kappa beta (NF-κβ) (reviewed in (Henderson et al., 2013)). The 26 amino acids at the N-terminus of HSP60 drives this protein to the mitochondria (Singh et al., 1990). Since VP8 was detected in both cytoplasm and mitochondria, the interaction of VP8 with HSP60 in the cytoplasm might serve to guide VP8 to mitochondria, or alternatively, VP8 might move to the mitochondria independently to interact with HSP60, thereby interfering with the maintenance of the MMP. HSP60 is localized to the mitochondrial matrix (Gupta and Austin, 1987) (Singh et al., 1990), and thus, VP8 is most likely co-localized in this compartment of the mitochondria. In addition, the presence of a mitochondrial targeting peptide in VP8 was examined by TargetP1.1 server, which is used to determine the subcellular localization of proteins (Emanuelsson et al., 2000). Hepatitis B virus X protein (HBX), a known viral mitochondrial protein, forms a complex with HSP60 and induces mitochondria-mediated apoptosis (Shirakata and Koike, 2003; Takada et al., 1999; Tanaka et al., 2004). The score for the presence of a mitochondrial targeting peptide in HBX was 0.43, whereas this score was 0.37 for VP8. Thus, VP8 might possess a mitochondrial targeting peptide, which might also facilitate import of VP8 into mitochondria.

Incubation of VP8-transfected cells with cytochrome C-specific antibody demonstrated that VP8 co-localized with cytochrome C. Due to the reduced MMP cytochrome C appeared to be partially released into the cytosol; this can trigger caspase activation (Liu et al., 1996) and agrees with the ability of VP8 to induce caspase activation (Afroz et al., 2018).

The localization of VP8 to the mitochondria correlated to mitochondrial dysfunction as determined by the reduction of MMP and ATP levels. Mitochondria are vital organelles to regulate cellular functions, and targeting mitochondria is a widely known strategy that viruses use for their survival, replication, and escape from the cells. For instance, hepatitis C virus (HCV) proteins localize to mitochondria where their function is impaired through reduction in MMP and increase of reactive oxidative stress (ROS) during productive infection (Piccoli et al., 2006). Similarly, human immunodeficiency virus (HIV) Vpr is targeted to mitochondria, facilitates reduction of MMP (Azuma et al., 2006), and promotes release of cytochrome C, which triggers apoptosis (Jacotot et al., 2000). Another viral protein, HBV X, interacts with HSP60 as well as with mitochondria (Tanaka et al., 2004), causes mitochondrial aggregation (Takada et al., 1999), and triggers cytochrome C release, which induces apoptosis (Kim et al., 2008). Furthermore, HBX reduces the MMP to trigger mitochondria-dependent cell death (Shirakata and Koike, 2003).

During BoHV-1 infection, VP8 was detected in the mitochondria at 2 h and continued to be localized to the mitochondria till at least 14 h post infection. While the MMP was reduced at 14 h after BoHV-1

infection, no reduction of MMP was observed at 2 or 4 h post infection. This is consistent with the fact that cellular MMP is maintained in HSV-1 infected cells till 6 h post infection, but reduced later after infection (Murata et al., 2000). HSV-1 tegument proteins, U_L41 and U_L46, are also associated with mitochondria, and the authors suggested that these tegument proteins migrate to the peri-nuclear region with mitochondria (Murata et al., 2000).

HSP60 maintains the MMP, as down-regulation of HSP60 reduces cellular MMP (Ghosh et al., 2010). Proper maintenance of MMP is associated with a normal level of ATP production. Any changes in the MMP level reduces ATP production (Bagkos et al., 2014). In agreement with the fact that VP8 expression decreased cellular MMP, a reduction in the ATP production was also observed in the presence of VP8. Additionally, during BoHV-1 infection, VP8 reduced MMP and ATP concentrations, whereas BoHV-1ΔU_L47 did not influence MMP and the ATP levels. These observations suggest a role of VP8 in perturbing mitochondrial function during infection by reducing MMP and ATP levels. In agreement with these results, BoHV-1 infection is known to induce mitochondrial dysfunction through reducing MMP, increasing oxidative stress and reducing ATP levels (Zhu et al., 2016), which can now be (partially) ascribed to VP8.

In conclusion, we report a new role for the multifunctional protein, VP8 of BoHV-1. VP8 interacted with HSP60, which may facilitate translocation of VP8 to mitochondria. In addition, or alternatively, the interaction of VP8 with HSP60 may prevent it from maintaining the MMP, which results in reduced ATP production and mitochondrial dysfunction during BoHV-1 infection.

Acknowledgements

We acknowledge Dr. Ravendra Garg for his technical assistance in FACS reading. We also acknowledge Scott Gradia for the pET His6 Sumo TEV LIC cloning vector (Addgene plasmid # 29659). The grant 90887-2010 RGPIN from the Natural Sciences and Engineering Research Council of Canada supported this research. SA was partially supported by a Canadian Institutes of Health Research Training Grant in Health Research Using Synchrotron Techniques (CIHR-THRUST). This is VIDO manuscript number 847.

References

Afroz, S., Brownlie, R., Fodje, M., van Drunen Littel-van den Hurk, S., 2016. VP8, the Major tegument protein of bovine herpesvirus 1, interacts with cellular STAT1 and inhibits interferon Beta signaling. J. Virol. 90, 4889–4904.

Afroz, S., Garg, R., Fodje, M., van Drunen Littel-van den Hurk, S., 2018. The Major tegument protein of bovine herpesvirus 1, VP8, interacts with DNA damage response proteins and induces apoptosis. J. Virol. 92 E00773-18.

Azuma, A., Matsuo, A., Suzuki, T., Kurosawa, T., Zhang, X., Aida, Y., 2006. Human immunodeficiency virus type 1 Vpr induces cell cycle arrest at the G(1) phase and apoptosis via disruption of mitochondrial function in rodent cells. Microbes Infect. 8, 670–679.

Bagkos, G., Koufopoulos, K., Piperi, C., 2014. A new model for mitochondrial membrane potential production and storage. Med. Hypotheses 83, 175–181.

Braig, K., Otwinowski, Z., Hegde, R., Boisvert, D.C., Joachimiak, A., Horwich, A.L., Sigler, P.B., 1994. The crystal structure of the bacterial chaperonin GroEL at 2.8 a. Nature 371, 578–586.

Bukau, B., Horwich, A.L., 1998. The Hsp70 and Hsp60 chaperone machines. Cell 92, 351–366.

Carpenter, D.E., Misra, V., 1991. The most abundant protein in bovine herpes 1 virions is a homologue of herpes simplex virus type 1 UL47. J. Gen. Virol. 72 (Pt 12), 3077–3084.

Castanier, C., Arnoult, D., 2011. Mitochondrial localization of viral proteins as a means to subvert host defense. Biochim. Biophys. Acta 1813, 575–583.

Chadha, P., Sarfo, A., Zhang, D., Abraham, T., Carmichael, J., Han, J., Wills, J.W., 2017. Domain interaction studies of herpes simplex virus 1 tegument protein UL16 reveal its interaction with mitochondria. J. Virol. 91 E01995-16.

Devireddy, L.R., Jones, C.J., 1999. Activation of caspases and p53 by bovine herpesvirus 1 infection results in programmed cell death and efficient virus release. J. Virol. 73, 3778–3788.

Emanuelsson, O., Nielsen, H., Brunak, S., von Heijne, G., 2000. Predicting subcellular localization of proteins based on their N-terminal amino acid sequence. J. Mol. Biol. 300, 1005–1016.

Ghosh, J.C., Siegelin, M.D., Dohi, T., Altieri, D.C., 2010. Heat shock protein 60 regulation of the mitochondrial permeability transition pore in tumor cells. Cancer Res. 70, 8988–8993.

Gupta, R.S., Austin, R.C., 1987. Mitochondrial matrix localization of a protein altered in mutants resistant to the microtubule inhibitor podophyllotoxin. Eur. J. Cell Biol. 45, 170–176.

Gupta, S., Knowlton, A.A., 2005. HSP60, Bax, apoptosis and the heart. J. Cell. Mol. Med. 9, 51–58.

Henderson, B., Fares, M.A., Lund, P.A., 2013. Chaperonin 60: a paradoxical, evolutionarily conserved protein family with multiple moonlighting functions. Biol. Rev. Camb. Philos. Soc. 88, 955–987.

Houry, W.A., Frishman, D., Eckerskorn, C., Lottspeich, F., Hartl, F.U., 1999. Identification of in vivo substrates of the chaperonin GroEL. Nature 402, 147–154.

Islam, A., Schulz, S., Afroz, S., Babiuk, L.A., van Drunen Littel-van den Hurk, S., 2015. Interaction of VP8 with mRNAs of bovine herpesvirus-1. Virus Res 197, 116–126.

Itoh, H., Komatsuda, A., Ohtani, H., Wakui, H., Imai, H., Sawada, K., Otaka, M., Ogura, M., Suzuki, A., Hamada, F., 2002. Mammalian HSP60 is quickly sorted into the mitochondria under conditions of dehydration. Eur. J. Biochem. 269, 5931–5938.

Jacotot, E., Ravagnan, L., Loeffler, M., Ferri, K.F., Vieira, H.L., Zamzami, N., Costantini, P., Druillennec, S., Hoebeke, J., Briand, J.P., Irinopoulou, T., Daugas, E., Susin, S.A., Cointe, D., Xie, Z.H., Reed, J.C., Roques, B.P., Kroemer, G., 2000. The HIV-1 viral protein R induces apoptosis via a direct effect on the mitochondrial permeability transition pore. J. Exp. Med. 191, 33–46.

Jones, C., Chowdhury, S., 2007. A review of the biology of bovine herpesvirus type 1 (BHV-1), its role as a cofactor in the bovine respiratory disease complex and development of improved vaccines. Animal Health Research Reviews / Conference of Research Workers in Animal Diseases 8, 187–205.

Kelly, B.J., Fraefel, C., Cunningham, A.L., Diefenbach, R.J., 2009. Functional roles of the tegument proteins of herpes simplex virus type 1. Virus Res 145, 173–186.

Kim, H.J., Kim, S.Y., Kim, J., Lee, H., Choi, M., Kim, J.K., Ahn, J.K., 2008. Hepatitis B virus X protein induces apoptosis by enhancing translocation of Bax to mitochondria. IUBMB Life 60, 473–480.

Labiuk, S.L., Babiuk, L.A., van Drunen Littel-van den Hurk, S., 2009. Major tegument protein VP8 of bovine herpesvirus 1 is phosphorylated by viral US3 and cellular CK2 protein kinases. J. Gen. Virol. 90, 2829–2839.

Latchman, D.S., 1988. Effect of herpes simplex virus type 2 infection on mitochondrial gene expression. J. Gen. Virol. 69 (Pt 6), 1405–1410.

Lin, Z., Rye, H.S., 2006. GroEL-mediated protein folding: making the impossible, possible. Crit. Rev. Biochem. Mol. Biol. 41, 211–239.

Liu, X., Kim, C.N., Yang, J., Jemmerson, R., Wang, X., 1996. Induction of apoptotic program in cell-free extracts: requirement for dATP and cytochrome c. Cell 86, 147–157.

Lobanov, V.A., Maher-Sturgess, S.L., Snider, M.G., Lawman, Z., Babiuk, L.A., van Drunen Littel-van den Hurk, S., 2010. A UL47 gene deletion mutant of bovine herpesvirus type 1 exhibits impaired growth in cell culture and lack of virulence in cattle. J. Virol. 84, 445–458.

Lund, K., Ziola, B., 1986. Synthesis of mitochondrial macromolecules in herpes simplex type 1 virus infected Vero cells. Biochem. Cell Biol. 64, 1303–1309.

Marblestone, J.G., Edavettal, S.C., Lim, Y., Lim, P., Zuo, X., Butt, T.R., 2006. Comparison of SUMO fusion technology with traditional gene fusion systems: enhanced expression and solubility with SUMO. Protein Sci. 15, 182–189.

Mettenleiter, T.C., Klupp, B.G., Granzow, H., 2009. Herpesvirus assembly: an update. Virus Res 143, 222–234.

Murata, T., Goshima, F., Daikoku, T., Inagaki-Ohara, K., Takakuwa, H., Kato, K., Nishiyama, Y., 2000. Mitochondrial distribution and function in herpes simplex virus-infected cells. J. Gen. Virol. 81, 401–406.

Osorio, J.S., Bionaz, M., 2017. Plasmid transfection in bovine cells: optimization using a realtime monitoring of green fluorescent protein and effect on gene reporter assay. Gene 626, 200–208.

Piccoli, C., Scrima, R., D'Aprile, A., Ripoli, M., Lecce, L., Boffoli, D., Capitanio, N., 2006. Mitochondrial dysfunction in hepatitis C virus infection. Biochim. Biophys. Acta 1757, 1429–1437.

Roizman, B., Carmichael, L.E., Deinhardt, F., de-The, G., Nahmias, A.J., Plowright, W., Rapp, F., Sheldrick, P., Takahashi, M., Wolf, K., 1981. Herpesviridae. Definition, provisional nomenclature, and taxonomy. The herpesvirus study group, the International committee on taxonomy of viruses. Intervirology 16, 201–217.

Shirakata, Y., Koike, K., 2003. Hepatitis B virus X protein induces cell death by causing loss of mitochondrial membrane potential. J. Biol. Chem. 278, 22071–22078.

Singh, B., Patel, H.V., Ridley, R.G., Freeman, K.B., Gupta, R.S., 1990. Mitochondrial import of the human chaperonin (HSP60) protein. Biochem. Biophys. Res. Commun. 169, 391–396.

Takada, S., Shirakata, Y., Kaneniwa, N., Koike, K., 1999. Association of hepatitis B virus X protein with mitochondria causes mitochondrial aggregation at the nuclear periphery, leading to cell death. Oncogene 18, 6965–6973.

Tanaka, Y., Kanai, F., Kawakami, T., Tateishi, K., Ijichi, H., Kawabe, T., Arakawa, Y., Kawakami, T., Nishimura, T., Shirakata, Y., Koike, K., Omata, M., 2004. Interaction of the hepatitis B virus X protein (HBx) with heat shock protein 60 enhances HBx-mediated apoptosis. Biochem. Biophys. Res. Commun. 318, 461–469.

Tsurumi, T., Lehman, I.R., 1990. Release of RNA polymerase from vero cell mitochondria after herpes simplex virus type 1 infection. J. Virol. 64, 450–452.

van Drunen Littel-van den Hurk, S., Garzon, S., van den Hurk, J.V., Babiuk, L.A., Tijssen, P., 1995. The role of the major tegument protein VP8 of bovine herpesvirus-1 in infection and immunity. Virology 206, 413–425.

Vasilenko, N.L., Snider, M., Labiuk, S.L., Lobanov, V.A., Babiuk, L.A., van Drunen Littel-van den Hurk, S., 2012. Bovine herpesvirus-1 VP8 interacts with DNA damage binding protein-1 (DDB1) and is monoubiquitinated during infection. Virus Res 167, 56–66.

Vassilev, V.B., Collett, M.S., Donis, R.O., 1997. Authentic and chimeric full-length genomic cDNA clones of bovine viral diarrhea virus that yield infectious transcripts. J. Virol. 71, 471–478.
Verhagen, J., Hutchinson, I., Elliott, G., 2006. Nucleocytoplasmic shuttling of bovine herpesvirus 1 UL47 protein in infected cells. J. Virol. 80, 1059–1063.
Watkins, A.M., Wuo, M.G., Arora, P.S., 2015. protein-protein interactions mediated by helical tertiary structure motifs. J. Am. Chem. Soc. 137, 11622–11630.
Xu, X., Zhang, K., Huang, Y., Ding, L., Chen, G., Zhang, H., Tong, D., 2012. Bovine herpes virus type 1 induces apoptosis through Fas-dependent and mitochondria-controlled manner in Madin-Darby bovine kidney cells. Virol. J. 9, 202.
Zeilstra-Ryalls, J., Fayet, O., Georgopoulos, C., 1991. The universally conserved GroE (Hsp60) chaperonins. Annu. Rev. Microbiol. 45, 301–325.
Zhang, S.M., Sun, D.C., Lou, S., Bo, X.C., Lu, Z., Qian, X.H., Wang, S.Q., 2005. HBx protein of hepatitis B virus (HBV) can form complex with mitochondrial HSP60 and HSP70. Arch. Virol. 150, 1579–1590.
Zhang, K., Afroz, S., Brownlie, R., Snider, M., van Drunen Littel-van den Hurk, S., 2015. Regulation and function of phosphorylation on VP8, the major tegument protein of bovine herpesvirus 1. J. Virol. 89, 4598–4611.
Zheng, C., Brownlie, R., Babiuk, L.A., van Drunen Littel-van den Hurk, S., 2004. Characterization of nuclear localization and export signals of the major tegument protein VP8 of bovine herpesvirus-1. Virology 324, 327–339.
Zhu, L., Yuan, C., Zhang, D., Ma, Y., Ding, X., Zhu, G., 2016. BHV-1 induced oxidative stress contributes to mitochondrial dysfunction in MDBK cells. Vet. Res. 47, 47.